A method for the measurement and interpretation of neuronal interactions: improved fitting of cross-correlation histograms using 1D-Gabor Functions

Ana-Maria Ichim
Transylvanian Institute of Neuroscience
Ploiești 33, Cluj-Napoca
Technical University of Cluj-Napoca
Email: am.ich@aol.com

Adriana Nagy-Dăbâcan
Transylvanian Institute of Neuroscience
Ploiești 33, Cluj-Napoca
Email: dabacan@tins.ro

Raul C. Muresan
Transylvanian Institute of Neuroscience
Ploiești 33, Cluj-Napoca
Email: muresan@tins.ro

***Abstract*—Cross-correlation analysis of separable multi-unit activity is the most used method to investigate neuronal connectivity. Features such as peaks, troughs, and satellite peaks in the cross-correlogram reflect the temporal relation between the activities of neurons. Precise estimation of such features requires independent measures. A very popular and effective method is to perform curve fitting using 1D Gabor functions. However, because of the non-linearity of the function, an iterative fitting procedure using optimization algorithms is required. As proposed from literature, we used the Levenberg-Marquardt algorithm. However, when applied to our data, the algorithm performed poorly. Here, we show that Trust Region algorithm represent a more attractive alternative to Levenberg-Marquardt in terms of performance and computational cost.**

***Index Terms*—1D-Gabor function, Levenberg-Marquardt algorithm, Trust-Region algorithm, cross-correlation, signal processing, spike sorting.**

I. Introduction

Interactions between neurons represent the building blocks of information processing in the brain. It is now recognized that the precise time delay between firing of neurons is fundamental in neural coding [1], synchrony [2], neuronal plasticity [3], and input integration [4]. The most common and effective method for estimating neuronal delays is to use a cross-correlation histogram (CCH). The CCH is a basic tool designed to compare time-related firing of neurons. When applied to a pair of spike trains, the CCH is the superposition of the firing time differences [5]. Features such as peaks, troughs and satellite peaks of the CCH are of most interest. For example, peaks at zero delay are taken as an evidence for common or correlated firing of the recorded neurons [6], [7]. The shape of CCH also caries information about dynamics of local circuits [8]. An interesting study designed by [8] has shown that cross correlation strength (e.g., ratio of the amplitude to the offset) was highest among cells with similar spatial tuning and similar temporal profile of activation. Furthermore, when presenting coherent stimuli, neurons tend to engage in a synchronous dance, exhibiting oscillatory firing patterns [9], [10] which are reflected in the CCH: a center peak flanked by oscillatory side lobes reflecting the temporal profile of discharge [9].

In order to quantify CCH features, several methods have been developed [11]. These methods, however, most of the time are statistically limited, as they consider each bin as an independent Poisson variable or as a normal approximation of it [11], [12] and therefore, run smoothly only when the sample size is substantial. Situations where one or both of the paired neurons fire a few spikes per trial produce ”noisy” CCHs, making it difficult, if not impossible, to estimate their features. Another fact that has to be considered when analyzing features of CCHs regard the bin size. Most of the studies investigating neuronal interactions bin the spike trains at 1 ms [9], [13]. However, recent studies have evidenced that neuronal delays can be measured with sub-millisecond precision [14]. For these reasons when measuring and interpreting CCH features caution is required. Methods using smoothing kernels for continuous cross-correlogram [5] and curve fitting (e.g., cosine, Gabor) [15], [9] have been proposed. In particular, fitting a Gabor function to CCHs represents a satisfactory and an efficient method for the measurement of neuronal delays. This is justified by the fact that experimentally computed CCHs on pairs of synchronized neurons exhibit similar features of a Gabor function: a central peak flanked by potential oscillatory side lobes.

In our experimental setup, we wanted to quantify the time delay between the firing of excitatory and inhibitory populations *in vivo* with millisecond and sub-millisecond precision. Therefore, we adapted the method proposed in [9]. We first fit the generalized Gabor function to a set of computed CCHs. As the function is nonlinear, for a good fit, an iterative process using optimization algorithms was necessary. For this propose, we used the Levenberg-Marquardt algorithm (LM) [16] as suggested in [9]. However, when applied to our data, the

978-1-7281-4914-1/19/$31.00

algorithm returned an optimal set of fitted parameters with real and imaginary parts. We therefore examined attentively the generalized Gabor function and noticed that in order to be solved in a real domain, the fitted parameters should satisfy some constraints. As the standard LM don't handle bound constraints we used the Trust Region algorithm (TR), [17] which is one of the most efficient algorithms in the area of constrained nonlinear optimization.

II. Methods

Data acquisition

The neurophysiological data used in this study was recorded from isoflurane anesthetized mice bred in the facilities of Transylvanian Institute of Neuroscience. Experiments have been performed in accordance with the Society for Neuroscience guidelines, Romanian law, and the European Communities Council Directive 2010/63/EU regarding the care and use of animals for experimental procedures. Experiments were approved by the Local Ethics Committee (3/CE/02.11.2018) and the National Veterinary Authority (ANSVSA; 147/04.12.2018).

Experimental design

Data were recorded by inserting a silicone A4x2 tetrode from Neuronexus in the visual cortex of the mice. Each probe consisted of four 5 mm long shanks adding up to 32 electrodes with a diameter of 50 μm. For visual stimulation, a monitor of 25x41 cm, with a resolution of 1440x900px and frame rate of 60 Hz was positioned in front of the animal. Stimuli consisted in drifting sinusoidal gratings with variable contrast and 8 different moving directions presented over 240 trials for each experimental session.

Signal Processing

The signal recorded from the 32 electrodes was amplified, processed and digitized with a sampling frequency of 32 KHz (*see figure 1*).

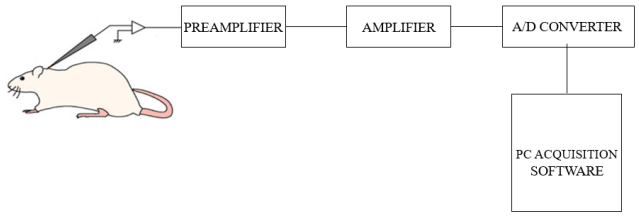

Fig. 1: **Acquisition chain:** Once the probe is inserted in the animal's brain, the neural signal picked up from the 32 contacts is transmitted to a preamplifier to remove noise contamination and further to an amplifier. Subsequently, it is digitized and managed by the acquisition software.

In order to extract spiking activity, the raw recorded signal was filtered using a 3^{th}order Butterworth filter, with a pass-band from 300 to 3000 Hz.

Spike Sorting

The process of spike sorting consisted in 3 main steps: spike detection, feature extraction and cluster analysis. Firstly, neural spikes were detected using an amplitude threshold [18]. With large number of channels, an automatic threshold computed as the standard deviation of the signal is preferable [19]. As suggested in [19], [18] the threshold was

$$Thr = 5n \tag{1}$$

where n is an estimation of the standard deviation of the signal.

Feature extraction was performed using Principal Component Analysis (PCA) with *K*-dimensional space set to 3. The resulting extracted features served as an input for the clustering procedure in which, we classified and assigned neuronal spikes corresponding to different neurons using the unsupervised *K-means* algorithm [20].

Fitting models to experimental data

In order to optimally estimate the features of the computed CCHs, we chose the Gabor function as our best curve fit [9]. The function is a sinusoidal plane wave modulated by a Gaussian envelope (*see figure 2*) and its 2D dimensional extension has been widely used in several computer vision applications such as visual and object recognition [21], feature extraction [22] and image segmentation [23].

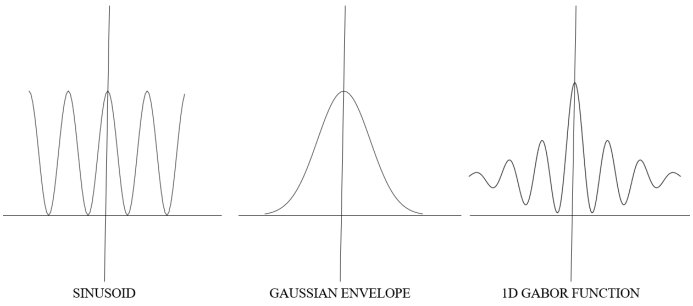

Fig. 2: **1D Gabor function:** Constituent elements of a 1D Gabor function.

Given a set of 8 variable parameters, we adapted from [9] the generalized Gabor function as follows :

$$\begin{aligned} CF(t) = Aexp(-(|t-\phi|/\sigma_1)^{\lambda})cos(2\pi\upsilon(t-\phi)) \\ + O + Bexp(-((t-\phi)/\sigma_2)^2) \end{aligned} \tag{2}$$

where A is the amplitude, ϕ is the phase change, σ_1 is the decay constant, υ is the temporal frequency, O is the offset, λ is the exponent, B is the central modulation coefficient, σ_2 is the width of the central peak. Each parameter can be described upon its influence on the function. Features such as phase, bandwidth, and frequency of the sinusoid in the envelope are shaped by ϕ, σ_1, and υ respectively. The central peak of the envelope is modeled by different values of the

exponent λ whereas features such as height and width are given by B and σ_2. To ensure the symmetry of the function with respect to the phase change, we added ϕ in the last term in the sum. Subsequently, we verified the existence-conditions of the function that satisfy the solution in real numbers. The function is not defined for σ_1, σ_2 equal to zero and for negative values of σ_1.

Optimization algorithms

Let (2) be the equation of a generalized (non-linear) Gabor function for the parameters λ, ϕ, σ, and υ. In order to achieve the best fit, an iterative process is needed. For this, we applied the (TR) algorithm which represents an alternative to (LM) method used in [9]. Although both methods are Newton step-based, TR exhibits better performance and more robustness to initial parameters [24]. Consider a general optimization problem defined as:

$$\min_{x \in \mathcal{X}} f(x),$$

where $f(x)$ is the objective function and $\mathcal{X} \subset \mathbb{R}^n$ the feasible region. The TR is an iterative method that starts by considering an initial solution in $\mathcal{X}$. At a given iteration k, TR solves a trust region sub-problem defined on a neighborhood of the current solution and in which the objective function is approximated by a simpler function (e.g., quadratic). More formally, this subproblem can be written as:

$$\begin{aligned} x_k^* &= \min_{d \in \mathcal{X}_k} m_k(d) \\ \text{s.t. } &\|d\|_{W_k} \leq \delta_n, \end{aligned}$$

where $m_k(d)$ is an approximation of the objective function $f(x_k + d)$ in a neighborhood of the iteration point x_k, $\mathcal{X}_k$ approximates the set $\mathcal{X} - x_k$, $\|d\|_{W_k}$ is a norm in $\mathbb{R}^n$, and δ_k is the radius of the trust region at iteration k [17]. If the new solution from this subproblem x_k^* is better than the current iterate x_k, it is accepted. The trust region can then be potentially updated in the next step (e.g., expanded or contracted; see [17] for more details).

$$f(x) = x^2 \tag{3}$$

III. Experimental results

This section provides an experimental comparison regarding the use of the LM and TR algorithms for solving the curve-fitting problem. Both optimization algorithms were implemented into the MATLAB function *lsqcurvefit*. Optimization options [25] are shown in table I.
All analysis run on Intel(R)@3.80GHz i7-7700HQ CPU.

TABLE I: Optimization options.

FunctionTolerance	1.0000e-06
MaxFunctionEvaluations	10000
MaxIterations	10000
StepTolerance	1.0000e-06
OptimalityTolerance	1.0000e-06

Validity and performance of the fitting process was tested on a set of 700 CCHs. The CCHs were computed for time shifts between -80ms and +80ms with a temporal resolution of 1 ms [9]. To assess goodness of fit we used χ^2. As LM and TR are algorithms to search local minima, the choice of initial values for the parameters is crucial. In order to achieve the best fit possible, we randomized 10 times the initial-values of ϕ and υ and then chose the fit with the lowest χ^2.

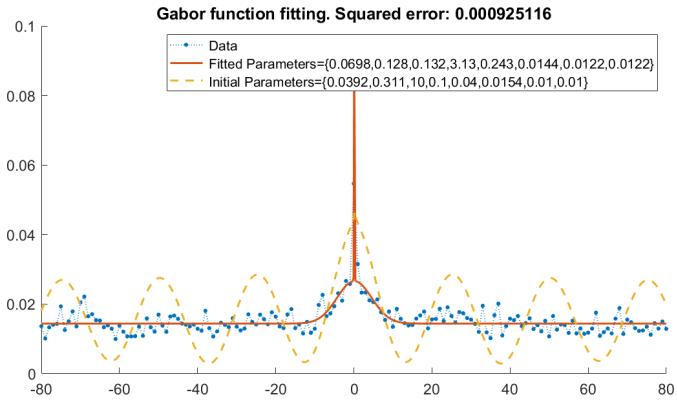

Fig. 3: **Gabor function fitting with LM algorithm**

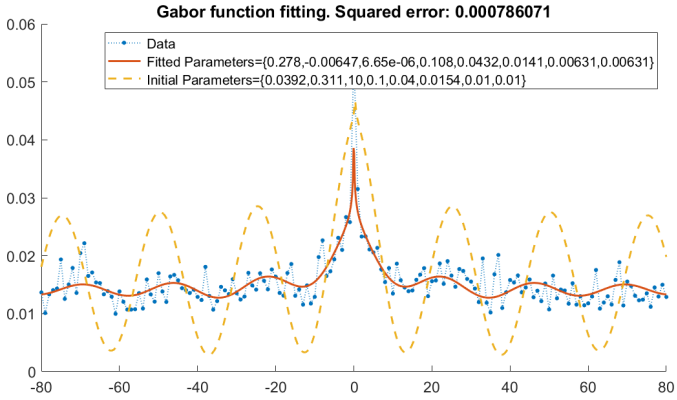

Fig. 4: **Gabor function fitting with TR algorithm**

Figure 3 and figure 4 show an oscillatory and synchronous CCH fitted (red straight line) with LM and TR respectively. The blue dots represent our CCH measured data. The initial parameters representing a generalized Gabor function is given by the yellow discontinuous line. By examining the plots it is evident that the best fit is achieved using TR algorithm. Furthermore, compared to LM, the value of the χ^2 is lower in TR. However, the comparison of χ^2 for all 700 CCHs (table II, last column) with LM and TR revealed that on average, both algorithms converged to almost identical solutions.

Table II illustrates a few statistics regarding the optimization process for both algorithms. Each value in the table represents an average for the 700 CCHs. OutputIterations consists in the numbers of the iterations needed for convergence. OutputFunc-Count represents the number of function evaluations [25]. It is

TABLE II: Statistics about the optimization process

Algorithm	OutputIterations	OutputFuncCount	χ^2
LM *unconstrained*	$794,029$	$768,7543$	$0,0424$
TR *constrained*	$62,0300$	$567,2700$	$0,0425$

apparent here that TR algorithm converges in considerably less iterations requiring fewer function evaluations. The difference in performance between the two algorithms could be explained by the fact that when a LM step fails, every update in the damping term λ [26] requires a new solution for the augmented equations therefore failed steps imply unproductive effort (see [26] for more details). On the contrary, TR requires less computational effort as it can solve the constrained subproblem for various values of δ_k [26].

IV. Concluding remarks

Cross-correlation analysis represents a valid and effective method for the estimation of neuronal delays. However, independent methods for the quantification of CCH features such as peaks, troughs, and satellite peaks are required. Our results show that fitting a 1D Gabor function to CCHs represents a robust and an efficient method for the quantification of CCH features. However, as the function is nonlinear, for a good fit, iterative processes using optimization algorithms such as LM or TR are required. We have compared the two methods and concluded that the overall performance of the minimization process is more reliable with TR. When applied to our data, LM performed poorly returning values of fitted parameters with imaginary parts. The reason is that the fitted Gabor function has no real solution for σ_1, σ_2 equal to zero and for negative values of σ_1. Consequently, some constraints should be satisfied before the iterative process. As the standard LM doesn't handle bound constraints, TR represented the perfect alternative for our case. TR returned real solutions that are the same quality of those to LM. Furthermore, by using TR, the computational cost of finding the best fit was reduced considerably.

Acknowledgments

This work was supported by: two grants from the Romanian National Authority for Scientific Research and Innovation, CNCS-UEFISCDI (Project Numbers PN-III-P4-ID-PCE-2016-0010 and COFUND-NEURON-NMDAR-PSY), and a National Science Foundation grant NSF-IOS-1656830 funded by the U.S. Government.

References

[1] E. T. Rolls and A. Treves, "The neuronal encoding of information in the brain," *Progress in neurobiology*, vol. 95, no. 3, pp. 448–490, 2011.

[2] W. Singer, "Neuronal synchrony: a versatile code for the definition of relations?" *Neuron*, vol. 24, no. 1, pp. 49–65, 1999.

[3] G.-q. Bi and M.-m. Poo, "Synaptic modifications in cultured hippocampal neurons: dependence on spike timing, synaptic strength, and postsynaptic cell type," *Journal of neuroscience*, vol. 18, no. 24, pp. 10 464–10 472, 1998.

[4] Z. F. Mainen and T. J. Sejnowski, "Reliability of spike timing in neocortical neurons," *Science*, vol. 268, no. 5216, pp. 1503–1506, 1995.

[5] I. Park, A. R. Paiva, T. B. DeMarse, and J. C. Príncipe, "An efficient algorithm for continuous time cross correlogram of spike trains," *Journal of Neuroscience methods*, vol. 168, no. 2, pp. 514–523, 2008.

[6] K. Toyama, M. Kimura, and K. Tanaka, "Cross-correlation analysis of interneuronal connectivity in cat visual cortex." *Journal of Neurophysiology*, vol. 46, no. 2, pp. 191–201, 1981.

[7] B. Lee, B. Cleland, and O. Creutzfeldt, "The retinal input to cells in area 17 of the cat's cortex," *Experimental brain research*, vol. 30, no. 4, pp. 527–538, 1977.

[8] C. Constantinidis, M. N. Franowicz, and P. S. Goldman-Rakic, "Coding specificity in cortical microcircuits: a multiple-electrode analysis of primate prefrontal cortex," *Journal of Neuroscience*, vol. 21, no. 10, pp. 3646–3655, 2001.

[9] P. König, "A method for the quantification of synchrony and oscillatory properties of neuronal activity," *Journal of neuroscience methods*, vol. 54, no. 1, pp. 31–37, 1994.

[10] A. K. Engel, P. König, A. K. Kreiter, and W. Singer, "Interhemispheric synchronization of oscillatory neuronal responses in cat visual cortex," *Science*, pp. 1177–1179, 1991.

[11] M. Abeles, "Quantification, smoothing, and confidence limits for single-units' histograms," *Journal of neuroscience methods*, vol. 5, no. 4, pp. 317–325, 1982.

[12] K. Graham and J. Duffin, "Cross correlation of medullary expiratory neurons in the cat," *Experimental neurology*, vol. 73, no. 2, pp. 451–464, 1981.

[13] C. M. Gray, P. König, A. K. Engel, and W. Singer, "Oscillatory responses in cat visual cortex exhibit inter-columnar synchronization which reflects global stimulus properties," *Nature*, vol. 338, no. 6213, p. 334, 1989.

[14] M. N. Havenith, A. Zemmar, S. Yu, S. M. Baudrexel, W. Singer, and D. Nikolić, "Measuring sub-millisecond delays in spiking activity with millisecond time-bins," *Neuroscience letters*, vol. 450, no. 3, pp. 296–300, 2009.

[15] E. N. Brown, R. E. Kass, and P. P. Mitra, "Multiple neural spike train data analysis: state-of-the-art and future challenges," *Nature neuroscience*, vol. 7, no. 5, p. 456, 2004.

[16] H. Gavin, "The levenberg-marquardt method for nonlinear least squares curve-fitting problems," *Department of Civil and Environmental Engineering, Duke University*, pp. 1–15, 2011.

[17] Y.-x. Yuan, "Recent advances in trust region algorithms," *Mathematical Programming*, vol. 151, no. 1, pp. 249–281, 2015.

[18] H. G. Rey, C. Pedreira, and R. Q. Quiroga, "Past, present and future of spike sorting techniques," *Brain research bulletin*, vol. 119, pp. 106–117, 2015.

[19] C. Pouzat, O. Mazor, and G. Laurent, "Using noise signature to optimize spike-sorting and to assess neuronal classification quality," *Journal of neuroscience methods*, vol. 122, no. 1, pp. 43–57, 2002.

[20] C. R. Caro-Martín, J. M. Delgado-García, A. Gruart, and R. Sánchez-Campusano, "Spike sorting based on shape, phase, and distribution features, and k-tops clustering with validity and error indices," *Scientific reports*, vol. 8, no. 1, p. 17796, 2018.

[21] C. Liu and H. Wechsler, "Gabor feature based classification using the enhanced fisher linear discriminant model for face recognition," *IEEE Transactions on Image processing*, vol. 11, no. 4, pp. 467–476, 2002.

[22] B. S. Manjunath and W.-Y. Ma, "Texture features for browsing and retrieval of image data," *IEEE Transactions on pattern analysis and machine intelligence*, vol. 18, no. 8, pp. 837–842, 1996.

[23] A. K. Jain and F. Farrokhnia, "Unsupervised texture segmentation using gabor filters," *Pattern recognition*, vol. 24, no. 12, pp. 1167–1186, 1991.

[24] F. V. Berghen, "Levenberg-marquardt algorithms vs trust region algorithms," *IRIDIA, Université Libre de Bruxelles*, 2004.

[25] J. Lofberg, "Yalmip: A toolbox for modeling and optimization in matlab," in *2004 IEEE international conference on robotics and automation (IEEE Cat. No. 04CH37508)*. IEEE, 2004, pp. 284–289.

[26] M. Lourakis and A. A. Argyros, "Is levenberg-marquardt the most efficient optimization algorithm for implementing bundle adjustment?" in *Tenth IEEE International Conference on Computer Vision (ICCV'05) Volume 1*, vol. 2. IEEE, 2005, pp. 1526–1531.